Structural Studies of the Palladium-Hydrogen System

A Thesis submitted for the Degree of
Doctor of Philosophy

By

Keith Gordon M^{c}Lennan

School of Science
Griffith University

August 2005

Statement

The thesis herein contains no material which has been submitted for a degree or diploma in any university, and to the best of my knowledge contains no material previously published or written by another person, except where due acknowledgment is made.

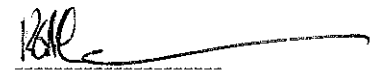

Keith M^{c}Lennan

Acknowledgements

Without whom, etc

The work in this thesis was begun in January 2000, and in the intervening five and half years I have received much help from colleagues, family and friends. I am convinced that completion of this thesis would have been much more difficult, if not impossible, without this help and so I set about now to thank them all.

I wish to thank my principal supervisor Associate Professor Evan Gray for guidance and help in all aspects of this work. Evan has taught me much about experimental methods and has provided good council over the years. He also has a good nose for restaurants, a much needed diversion in the middle of experimental runs.

Professor John Dobson, my co-supervisor, provided help with the Density Functional Theory parts, especially in organising access to computer resources.

I would like to thank both Evan and John for organizing a Griffith University School of Science Postgraduate Scholarship near the end of my tenure when it was much needed

My colleagues Dr Tomasz Blach and Dr Mark Pitt have both been a great help to me when preparing for experiments, especially early on during my transformation from theoretician to experimenter. They have also provided much-needed company during those long beam-time runs. Thanks specifically to Tom for showing me the fine art of "power sight-seeing", and to Mark for introducing the operation of the Rietica computer program to me

During the course of this research, I held an Australian Postgraduate Research award, supplemented with an Australian Institute of Nuclear Science and Engineering award I wish to thank my AINSE co-supervisor Dr Shane Howard for insightful help into some of the subtleties of Rietveld refinement. I thank AINSE for the financial support and for providing access to the HIFAR diffraction instruments.

In-situ diffraction studies are difficult experiments to perform successfully, and I need to thank all of the instrument scientists who have helped me complete mine. They are, in no particular order, Dr Brett Hunter and Dr Andrew Studer of the Bragg Institute at ANSTO, Dr Peter Fischer (retired) of the SINQ facility at the Paul Scherrer Institute and Kevin Knight of the ISIS facility at the Rutherford Appleton Laboratory. All of these

gentlemen have provided highly professional support during various experiments and their help was invaluable.

I would like to thank both Dr Erich Kisi and Dr Klaus Yvon for helping to improve my understanding of crystallography

Dr Chris Brown was very helpful in providing computer resources when they were most needed.

Finally, I need to thank my partner, Julie, and daughter, Lydia, for so much patience over the last few years. They have put up with my distractions, workload and many absences with good grace and courage. This thesis is dedicated to them.

Abstract

In this work the palladium-hydrogen system has been studied using experimental and computational techniques. The experimental technique used was in-situ neutron powder diffraction. The in-situ methodology, in which diffraction data are collected from a sample loaded to a known hydrogen concentration, provides an independent measure of the hydrogen occupation of interstitial lattice sites.

Theoretical modeling with the ADF-BAND software was done to calculate lattice parameters and investigate interstitial occupancy

An important driver for this work was a new report of occupation of tetrahedral interstices near the thermodynamic critical temperature, above which the hydriding phase transformation is continuous. The two-pronged approach was adopted to provide experimental input to the modeling and theoretical understanding of the experiments

The focus of the work carried out was the peri-critical region of the palladium-hydrogen system. While raising significant technical challenges to the experiments, this meant that modeling was made easier, as the system is single-phase above the critical temperature. Fairly direct comparisons of theory and experiment were therefore possible.

The experiments performed have revealed much new information about the previously well studied palladium-hydrogen system. Differences have been identified in some thermodynamic properties of this system based upon the bulk form of the palladium, whether solid sheet or finely divided. The two forms have different shapes to their pressure-composition isotherms, the form of the hysteresis is different and they display markedly different thermodynamic critical temperatures.

The determination of the thermodynamic critical temperature was also focused on. The classical method of determining critical temperature by the disappearance of the hysteresis in the pressure-composition-temperature (p-c-T) curves has proved to be inaccurate. Above the critical temperature, but still in the peri-critical region, where the hysteresis in the p-c-T curves proves undetectable, it is possible to distinguish two phases via diffraction pattern refinement. The nature of these phases is slightly different to the typical α and β phases located well below the critical temperature where the phases behave very differently. In the peri-critical region the two phases are very similar and each follows the Vegard relationship independently.

A significant part of the research was directed at the location of deuterium atoms in the palladium face centered cubic (FCC) lattice. Two sites in the FCC lattice are available to the deuterium, the tetrahedral site and the octahedral site, and traditionally it is thought that only the octahedral site is occupied. Based on fundamental calculations on peak heights, as well as on full Rietveld refinement, it has been shown that there is now compelling evidence for tetrahedral occupation in the peri-critical region of palladium-deuterium

The theoretical calculations performed accurately estimated the lattice parameters for the range of palladium-hydrogen stoichiometries. By enlarging the modeled unit cell, several hydrogen concentrations could be represented. These calculations provided support for the idea of tetrahedral site occupation by hydrogen of the palladium FCC lattice, and predicted the experimentally observed trend to higher tetrahedral occupancy in the middle of the concentration range Pd to PdH.

Table of Contents

Statement I

Acknowledgements II

Abstract IV

Table of Contents VI

List of Figures XI

Chapter One Thesis Overview

1.1 The Hydrogen Economy 2

1.2 The Problem of Hydrogen Storage 3

1.3 The Study of Palladium-Hydrogen 4

1.4 Thesis Structure 5

References 7

Chapter Two Materials and Methods

2.1 Introduction 9

2.2 Palladium 9

2.3 Hydrogen 10

2.4 Palladium-Hydrogen System 10

2.4.1 Characteristics of the Palladium Hydrogen System 11

2.4.2 The Palladium-Hydrogen Phase Diagram 11

2.4.3 The Palladium-Hydrogen Critical Temperature 12

2.4.4 Palladium and the Storage of Hydrogen 13

2.4.5 Palladium and the Separation of Hydrogen 14

2.5 Methods for Determining Hydrogen-to-Metal Ratios 15

2.5.1 The Gravimetric Technique 16

2.5.2 The Sieverts Technique 16

2.5.3 The Compressibility of Deuterium 19

2.5.4 The Hot-Cold Volume Model 21

2.6 Neutron-Beam Diffraction Instruments 22

2.6.1 The HIFAR MRPD Instrument 23

2.6.2 The HIFAR HRPD Instrument 23

2.6.3 The SINQ HRPT Instrument 25

2.6.4 The ISIS HRPD Instrument 26

2.7 Density Functional Theory 27

References 28

Chapter Three **In-situ Neutron-beam Diffraction Studies of the Palladium-Deuterium System: Macroscopic Properties**

3.1 Introduction 31

3.2 Sample Preparation 31

3.3 HIFAR MRPD October 2001 33

3.3.1 Manometrics: Supercritical Isotherm 34

3.3.2 Manometrics: Critical Isotherm 35

3.3.3 Manometrics: Subcritical Isotherm 37

3.3.4 The Peri-critical Region of the Palladium-Deuterium System 38

3.4 SINQ HRPT May 2002 39

3.4.1 Manometrics 39

3.5 HIFAR MRPD July 2002 41

3.5.1 Manometrics 41

3.5.2 Instrument Calibration Problems 42

3.6 HIFAR HRPD October 2003 44

3.6.1 Manometrics 44

3.7 ISIS HRPD March/April 2004 46

3.7.1 Issues Affecting the Proposed Beam-Time 46

3.7.2 Manometrics 47

3.7.3 The Pre-Dislocation 310°C Isotherm 52

3.7.4 The 120°C Isotherm 53

3.7.5 The Annealing Temperature Scans 54

3.7.6 The Post-Annealing 310°C Isotherm and Quench 55

3.8 Conclusions and Discussion 57

References 59

Chapter Four **In-situ Neutron-beam Diffraction Studies of the Palladium-Deuterium System: Lattice Parameters**

4.1 Introduction 62

4.2 Rietveld Analysis 64

4.3 HIFAR MRPD October 2001 65

4.3.1 Introduction 65

4.3.2 Refinement Problems 65

4.3.3 The Super-Critical Isotherm 65

4.3.4 The Critical Isotherm 67

4.3.5 The Sub-Critical Isotherm 68

4.3.6 The Peri-Critical Region Lattice Parameters 69

4.4 SINQ HRPT May 2002 70

4.4.1 Introduction 70

4.4.2 Lattice Parameters 70

4 5 HIFAR HRPD July 2002 71

4.5.1 Introduction 71

4.5.2 Refinement Problems 71

4.5.3 Lattice Parameters 71

4.6 HIFAR HRPD October 2003 73

4.7 ISIS HRPD March/April 2004 74

4.7.1 Introduction 74

4.7.2 The Lattice Parameters of the Pre-Dislocation 310°C Isotherm 75

4.7.3 The Lattice Parameters of the 120°C Isotherm 76

4.7.4 The Annealing Temperature Scan Patterns 77

4.7.5 The Post-Annealing Lattice Parameters 82

4.7.6 All ISIS HRPD Results 83

4.8 Comparison of All Results 84

4.9 Conclusions and Discussions 85

References 89

Chapter Five **In-situ Neutron-beam Diffraction Studies of the Palladium-Deuterium System: Deuterium Occupation of the Tetrahedral Site**

5.1 Introduction 91

5.2 Structure Factor Rules Governing the Octahedral and Tetrahedral Site Occupation of the FCC Lattice 93

5.3 A Comparison of the Calculated Peak Heights and the Experimentally Measured Peak Heights 102

5.4 Procedure for Analysing High Resolution Data 108

5.5 Refined Occupations 109

5.6 Conclusions and Discussions 113

References 115

Chapter Six **A Computational Study of the Peri-Critical Region of the Palladium-Hydride System Using Density Functional Theory Techniques**

6.1 Introduction 117

6.1.1 Density Functional Theory 118

6.1.2 The Hartree Approximation 118

6.1.3 Exchange and Correlation 119

6.2 Theory of ADF-BAND 119

6.3 Computational Technique 121

6.3.1 Unit Cells Used for Computations 122

6.3.2 Orbital Functions 125

6.4 Calculated Lattice Parameters 129

6.5 Octahedral and Tetrahedral Site Occupation 131

6.5.1 General Palladium-Hydrogen System Calculations 131

6.5.2 Detailed Calculations of Pd_8H_3 134

6.5.3 Energy Profile of the Cube Diagonals 136

6.6 Conclusions and Discussions 140

References 142

Summary 143

References

Appendix **Published Works** A-I

Prediction of Dispersion Forces: Is There a Problem?

An Equation of State for Deuterium gas to 1000 bar

Soft Cohesive Forces

List of Figures

Fig 2.1	The face-centered-cubic crystal structure	9
Fig 2.2	Palladium-protium p-c-T relationships and the palladium-protium phase diagram	12
Fig 2 3	Schematic of hydrogen separation in a palladium membrane	15
Fig 2.4	Experimental setup of an in-situ diffraction study	facing 16
Fig 2.5	The HRPD diffractometer	24
Fig 2 6	SINQ HRPT sample table	25
Fig 2.7	SINQ HRPT schematic	25
Fig 2.8	ISIS facility at RAL	26
Fig 3 1	Schematic of Sieverts apparatus used in October 2001	33
Fig 3.2	Pd-D Supercritical isotherm	35
Fig 3.3	Pd-D Supercritical diffraction patterns	35
Fig 3 4	Pd-D Critical isotherm	36
Fig 3 5	Pd-D Critical diffraction patterns	36
Fig 3.6	Pd-D Sub-critical isotherm	37
Fig 3 7	Pd-D Sub-critical diffraction patterns	37
Fig 3.8	The peri-critical region of palladium-deuterium	38
Fig 3.9	Pressure-composition isotherms for the palladium-deuterium bulk sheet sample	facing 39
Fig 3 10	Schematic of Sieverts apparatus used in May 2002 on SINQ HRPT	39

Fig 3.11 Neutron diffraction patterns from palladium-deuterium 40

Fig 3.12 Schematic of Sieverts apparatus used in July 2002 on HIFAR MRPD 41

Fig 3.13 Room temperature p-c-T diagram for palladium-deuterium 42

Fig 3.14 Room temperature neutron diffraction patterns of palladium-deuterium 42

Fig 3.15 Detail of diffraction patterns of palladium-deuterium collected on HIFAR MRPD July 2002 43

Fig 3.16 Schematic of Sieverts apparatus used on HIFAR HRPD October 2003 44

Fig 3.17 p-c-T diagram for palladium-deuterium 45

Fig 3.18 Diffraction patterns collected for palladium-deuterium on HIFAR HRPD October 2003 45

Fig 3.19 Schematic of Sieverts apparatus used on ISIS HRPD May 2004 47

Fig 3.20 Pressure-composition-temperature graph of palladium-deuterium 48

Fig 3.21 Palladium-deuterium isotherms facing 49

Fig 3.22 Neutron-beam diffraction patterns from palladium collected on ISIS HRPD 51

Fig 3.23 Palladium-deuterium isotherm at 310°C 52

Fig 3.24 Palladium-deuterium neutron diffraction patterns for 310°C isotherm collected on ISIS HRPD 52

Fig 3.25 Palladium-deuterium isotherm at 120°C 53

Fig 3.26 Palladium-deuterium neutron diffraction patterns collected ISIS HRPD, sample at 120°C 53

Fig 3.27 Palladium annealing temperature neutron diffraction patterns ISIS HRPD 55

Fig 3.28 Palladium annealing temperature neutron diffraction patterns ISIS HRPD (detail) 55

Fig 3.29 Palladium-deuterium 310°C isotherm and quench step 56

Fig 3.30 Palladium-deuterium neutron diffraction patterns collected ISIS HRPD 56

Fig 4.1 Supercritical isotherm (300°C), refined lattice parameter vs. deuterium content, absorption isotherm only 66

Fig 4.2 Critical isotherm (280°C), refined lattice parameter vs. deuterium content, absorption and desorption isotherms 67

Fig 4.3 Sub-critical isotherm (250°C), refined lattice parameter vs. deuterium content, absorption and desorption isotherms 68

Fig 4.4 Lattice parameters of the palladium-deuterium system near the peri-critical region facing 69

Fig 4.5 Refined lattice parameters vs. deuterium concentration at 295-320°C facing 70

Fig 4.6 Refined lattice parameters from room-temperature palladium-deuterium facing 71

Fig 4.7 Comparison of lattice parameters refined from experiments of October 2001 and July 2002 72

Fig 4.8 Refined lattice parameters of palladium-deuterium on HRPD HIFAR October 2003 73

Fig 4.9 Refined palladium-deuterium lattice parameters for 310°C isotherm 75

Fig 4.10 Refined lattice parameters from the 120°C isotherm facing 76

Fig 4.11 Critical and sub-critical lattice parameters 77

Fig 4.12 Annealing temperature lattice parameters 78

Fig 4.13 All pure palladium lattice parameters 78

Fig 4.14 Refined thermal parameter B during annealing 79

Fig 4.15 Refined peak-shape parameter γ_1 during annealing 79

Fig 4.16 Refined peak-shape parameter γ_2 during annealing 80

Fig 4.17 Refined particle size parameter A_{size} during annealing 80

Fig 4.18 Palladium-deuterium annealing experiment peak-shape parameters 81

Fig 4.19 Lattice parameters of the palladium-deuterium 310°C isotherm and quench 82

Fig 4.20 All results from ISIS HRPD March/April 2004 83

Fig 4.21 The lattice parameters of PdH_x and PdD_x from neutron diffraction studies 84

Fig 5.1 Location of the tetrahedral and octahedral sites in the face centered cubic structure 91

Fig 5.2 Palladium deuterium calculated peak heights of the three lowest order peaks on a time-of-flight neutron diffractometer using an octahedral occupation only model facing 103

Fig 5.3 Palladium deuterium relative peak heights of the three lowest order peaks for a time-of-flight neutron diffractometer using an octahedral occupation only model 104

Fig 5.4 Palladium deuterium relative peak heights of the three lowest order peaks for a constant-wavelength neutron diffractometer using an octahedral occupation only model 104

Fig 5.5 Relative peak height comparisons for a time-of flight neutron diffractometer, expected and experimental 105

Fig 5.6 Relative peak height comparisons for a constant wavelength neutron diffractometer, expected and experimental 106

Fig 5.7 Relative peak height comparisons for a constant-wavelength neutron diffractometer, expected and experimental 107

Fig 5.8 Palladium-deuterium system. Deuterium octahedral site and tetrahedral site occupation numbers near the system critical temperature. 110

Fig 5.9 Palladium-deuterium system Single-phase deuterium octahedral and tetrahedral site occupation numbers at 310°C 111

Fig 5.10 Thermal parameters of octahedral and tetrahedral located deuterium in palladium at 310°C 112

Fig 6.1 Primitive basis set for generating FCC structure. Single atom basis with rhombohedral translation axes 122

Fig 6.2 Cubic basis for generating the FCC structure Four atom basis with cubic translation axes 123

Fig 6.3 Double-cubic basis set for generating FCC structure. Eight atom basis with rectilinear translation axes 124

Fig 6.4 Calculated lattice parameters for Pd_xH 129

Fig 6.5 Calculated lattice parameters for PdxH compared to experimental results from this thesis 130

Fig 6.6 Palladium Hydride Energy of Formation - effect of moving hydrogen atoms from octahedral to tetrahedral sites 131

Fig 6 7 Palladium Hydride Fermi Energy - effect of moving hydrogen atoms from octahedral to tetrahedral sites 133

Fig 6 8 Pd8H3 Energy of Formation – octahedral/tetrahedral site occupation comparison 134

Fig 6.9 Nearest neighbour considerations for 8-atom rectilinear "double-cubic" unit cell 136

Fig 6 10 Energy of Formation Pd_2H facing 137

Fig 6 11 Fermi Energy Pd_2H facing 137

Fig 6.12 Energy of Formation Pd_2H facing 137

Fig 6.13 Fermi Energy Pd_2H facing 137

Fig 6 14 Energy of Formation Pd_2H – low symmetry configuration 138

Fig 6.15 Energy of Formation Pd_4H facing 139

Fig 6.16 Fermi Energy Pd_4H facing 139

Fig 6 17 Energy of Formation Pd_4H facing 139

Fig 6.18 Fermi Energy Pd_4H facing 139